

Boriding of Equiatomic Fe–Mn Binary Alloy

A. CALIK^a, Y. GENCER^b, M. TARAKCI^{b,*}, K.O. GUNDUZ^b AND A.E. GULEC^b

^aFaculty of Technology, Manufacturing Engineering, Suleyman Demirel University, Isparta, Turkey

^bGebze Institute of Technology, Department of Materials Science and Engineering, Gebze, Kocaeli, Turkey

Synthetic equiatomic Fe–Mn binary alloy was prepared under vacuum-argon controlled atmosphere. Fe–Mn alloy samples were boronized using the commercial Ekabor II powder at 900 °C, 1000 °C and 1100 °C for 3 h. The borided samples were characterized by X-ray diffraction, scanning electron microscopy–energy dispersive spectroscopy, and profilometry. The boride layers were composed of FeB, MnB, MnB₂ and Fe₂B phases for the samples borided at 1000 °C and 1100 °C while the sample borided at 900 °C was composed of only FeB and MnB. The boride layer was well adhered to the substrate with saw-tooth like morphology however some discontinuous band of cracks were observed in the boride layer. The concentration ratio of Fe and Mn were equal along the thickness of the coating though in some areas their ratio interchanged. The boride layer thickness and surface roughness increased with boronizing temperature.

DOI: 10.12693/APhysPolA.123.449

PACS: 81.15.-z, 81.05.Bx, 68.35.Fx

1. Introduction

Boronizing temperature, duration and chemical composition of the substrate are the main parameters affecting the properties of the boride layer formed during the boronizing process [1–8]. Besides the type of the substrate material itself, the alloying elements in substrate material directly affect the properties of boride layer [1, 2, 6–8]. There are limited studies about the effect of alloying elements on boronizing behaviour of steels [9–15]. Being an austenite stabilizing element, manganese is added to steels to improve mechanical properties and used up to 32 wt% in specific steels [16–21]. The effect of manganese on the boronizing behaviour of low carbon steel and Fe–Mn binary alloys containing less than 1 wt% Mn were reported [2, 17]. However results obtained from these studies are contradicting in terms of determining the morphology, microstructure and thickness of boride layers [2, 17].

Therefore another attempt was made to clarify the specific effect of Mn on boronizing behaviour of pure iron by adding 1–16 wt% Mn into pure iron [9]. Although in this study, thickness, interface morphology and microstructure of the boride layer were not significantly different compared to borided pure iron, the increasing Mn content prevented the crack formation between FeB and Fe₂B phases. This ineffectiveness of Mn was attributed to the similarities of iron and manganese both in atomic and crystal structure. Taking as a guide the similarities between iron and manganese, the aim of this study is whether the equal addition of iron and manganese will change the boride layer properties in comparison with the previous report.

For this purpose, equiatomic Fe–Mn alloy was prepared under controlled atmosphere, borided at 900 °C, 1000 °C and 1100 °C for 3 h and characterized using X-ray diffraction (XRD), optical microscopy (OM), scanning electron

microscopy–energy dispersive spectroscopy (SEM–EDS) and profilometry.

2. Experimental

Pure iron (99.97%) and pure manganese (99.9%) pieces were obtained from Alfa Aesar to prepare Fe–Mn alloy with equal amount of iron and manganese. The alloy was prepared by arc melting and solidified under controlled atmosphere. The arc-melting process was repeated at least six times to obtain chemically homogeneous Fe–Mn alloy. The samples with approximate dimensions of 10 mm × 10 mm × 2.5 mm were cut from the ingot. The plate shaped samples were ground using 320–1200 grit emery papers, polished using diamond paste and cleaned using acetone in an ultrasonic cleaner. Surface roughness (R_a) of the Fe–Mn alloy was measured by using Veeco Dektak 8 profilometer. The Fe–Mn alloy substrate was then embedded into commercial Ekabor II boronizing powder inside a ceramic crucible. Then the crucible was tightly sealed and loaded to a box furnace under atmospheric pressure. The boronizing process was carried out at 900 °C, 1000 °C and 1100 °C for 3 h.

The profilometry was performed to analyze surface roughness of the borided surface with the same parameters used for the bare substrates. Rigaku D-MAX 2200 X-ray diffractometer with a Cu K_α radiation over a 2θ range from 20° to 90° was used for the phase determination of boride coatings. Then the samples were cut into two pieces, mounted into epoxy resin, ground and polished for cross-sectional microstructure examination. Zeiss OM was employed for cross-sectional examination. The Philips XL30 SEM with EDS facility was used to examine the chemical composition of the borided samples from the cross-section of polished samples.

3. Results

Figure 1 shows the surface XRD examinations of borided (900 °C, 1000 °C, 1100 °C) Fe–Mn alloy. The

*corresponding author; e-mail: mtarakci@gyte.edu.tr

XRD spectrum revealed that the boride layer was composed of only FeB and MnB for boronized Fe–Mn alloy at 900 °C whereas boriding at 1000 °C and 1100 °C promoted the formation of Fe₂B and Mn₂B in addition to FeB and MnB phases observed in all specimens.

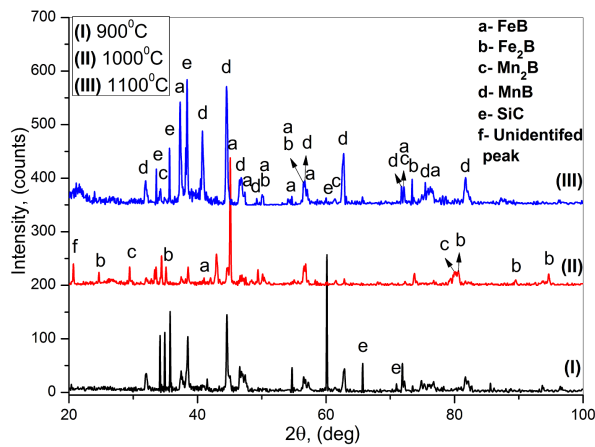


Fig. 1. XRD pattern from the surface of borided Fe–Mn.

The spectrum shows that there are peaks belong to SiC. The existence of the SiC was attributed to the boronizing powder bonded to the surface of the boride layer during boronizing. There is one unidentified peak which was marked as “X” in the spectrum.

Figure 2 shows cross-sectional OM micrographs of the borided Fe–Mn alloys at different temperatures (Fig. 2). It can be clearly seen from the figures that the borided layer well adhered to the substrates and the adhesion was supported with the saw tooth like morphology as the interface area is significantly high.

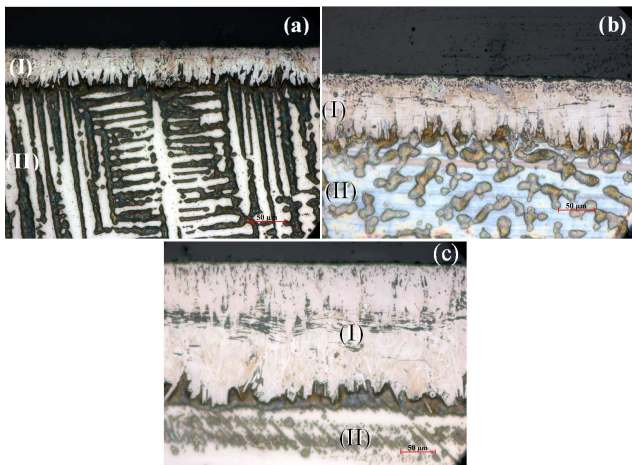


Fig. 2. Cross-sectional OM images of pack boronized Fe–Mn alloys: (a) 900 °C, (b) 1000 °C, and (c) 1100 °C. (I) Boride layer, (II) substrate.

However, the morphology is not purely saw tooth as in the case of low Mn containing Fe–Mn alloys [17].

The boride layer is mainly composed of two distinct phases or phase mixtures which can be distinguished from their contrast difference in cross-sectional SEM or OM examinations. It was usually reported in the literature that the outer dark region was FeB and inner lighter region was Fe₂B for the boronized ferrous materials [2, 9]. However, in this study XRD results show that the formation of MnB, Mn₂B along with FeB, Fe₂B formation was evident. So, it may be concluded that the outer dark region was composed of boron rich FeB and MnB phases while light coloured inner region was composed of Fe₂B and Mn₂B.

As reported in the literature, during the boronizing process firstly Fe₂B phase forms. Upon formation, the Fe₂B phase hinders the boron diffusion, therefore increasing the boron potential of the surface. Consequently, boron-rich FeB phase formation was favoured on the outer surface of the boride layer. It is possible to attribute the formation of MnB and Mn₂B to the same mechanism.

At low temperature neither Fe₂B nor Mn₂B phase was formed on the surface during boronizing of equiatomic Fe–Mn (Fig. 1) as boron diffusion was very low and only boron-rich phase formation was favoured on the surface.

It should not be ignored that the formation of Fe₂B and Mn₂B was evident in the inner region (Fig. 2). The outermost surface of the boride layer has finely distributed pores for all temperatures. The volume of the porosity increases with boriding temperature. It may be attributed to the volatile substances arisen during high temperature boriding process. Clear, discontinuous band of cracks were observed in the coating, which are parallel to boride layer surface. These cracks are mainly between the two distinct boride regions and their quantity has increased with boriding temperature. These cracks are formed most probably due to the differences between linear thermal expansion coefficients of the phases formed in the boride layer (Fig. 1) during the cooling stage after boronizing. Although much longer cracks were widely reported for the borided ferrous materials, the cracks for borided Fe–Mn in this study are much shorter in size [2]. It should be noted that in the previous study it was reported that the crack formation was avoided by high Mn addition into Fe [9].

Fe, Mn and B distribution obtained along the thickness of boride coating was shown in the SEM–EDS spectrum (Fig. 3b) along a line from the surface of boride layer to the substrate with cross-sectional SEM image (Fig. 3a) for borided Fe–Mn alloy at 1100 °C. The spectrum (Fig. 3b) shows that the concentration of Fe and Mn increases from the surface of boride layer towards the substrate with some scattering, yet their rational concentrations are approximately the same in the substrate and the boride layer. It should be noted that boride layer is either composed of Mn rich and Fe poor areas or vice versa. The boron concentration seems almost constant through the boride layer but its detection was difficult due to its small atomic number. However, the XRD re-

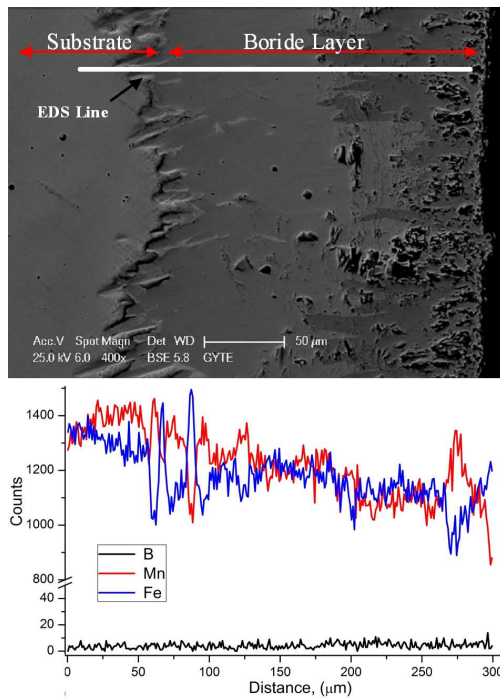


Fig. 3. Cross-sectional micrographs and EDS analysis of pack boronised Fe–Mn alloy at 1100 °C for 3 h.

sults confirmed that the coating layer consists of Mn–B and Fe–B phases or their mixture.

Figure 4 illustrates the boride layer thickness and surface roughness versus boriding temperature. Figure 4 revealed that boride layer thickness was increased with boronizing temperature from approximately 60 μm (900 °C) to 190 μm (1100 °C). This result is parallel to the findings of boronized ferrous materials that as the boronizing temperature increases boron diffusion increases and consequently boride layer thickness increases as reported in the literature. The figure also shows that the surface roughness (R_a) increased with boronizing temperature as it increased from 0.8 μm (900 °C) to 1.7 μm (1100 °C) while the surface roughness was 0.1 μm for the bare substrate before boronizing. The bonding of the boriding powders to the surface of boride layer as well as the pores formed due to volatile substances resulted in higher surface roughness at higher temperature.

4. Conclusions

The XRD spectrum reveals that the boride layer is composed of only FeB and MnB for boronized Fe–Mn alloy at 900 °C. The increase in boronizing temperature promotes the formation of Fe_2B and MnB_2 at the surface of boride layer as well in addition to FeB and MnB phases at 1000 °C and 1100 °C.

It is seen from the figures that the borided layer well adhered to the substrates and the adhesion was supported with the saw tooth like morphology as the interface area is significantly high. However, the morphology

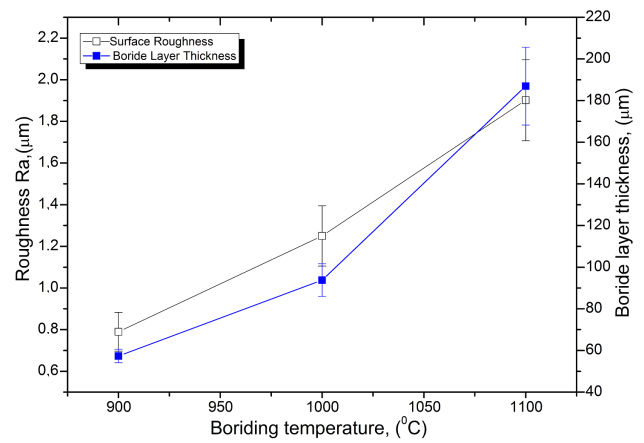


Fig. 4. The boride layer thickness and surface roughness (R_a) vs. boronizing temperature.

is not purely saw tooth as in the case of low Mn containing Fe–Mn alloys.

The outermost surface of the boride layers has finely distributed porous structure for all temperatures. The volume of the porosity increases with boriding temperature.

Clear, discontinuous band of cracks in the coating, which are parallel to boride surface, are seen for the borided Fe–Mn alloy. These cracks are mainly between the two distinct boride regions and increase in number with boriding temperature.

The spectrum shows that the concentration of Fe and Mn increases from the surface of boride layer towards the substrate with some scattering, though their rational concentrations are approximately the same in the substrate and the boride layer. It should be noted that boride layer is either composed of Mn rich and Fe poor areas or vice versa.

The boride thickness and surface roughness increased with boronizing temperature.

Acknowledgments

The author expresses his thanks to technicians Adem Sen and Ahmet Nazım for their kind assistance during XRD and SEM experimental studies.

References

- [1] I. Ozbek, C. Bindal, *Surf. Coat. Technol.* **154**, 14 (2002).
- [2] A.K. Sinha, in: *ASM International Handbook*, Vol. 4 *Heat Treating*, Materials Park (Oh) 1991 p. 437.
- [3] P.A.D.A.T. Bell, *Surf. Eng.* **1**, 203 (1985).
- [4] G. Palombarini, M. Carbucicchio, *J. Mater. Sci. Lett.* **3**, 791 (1984).
- [5] C. Martini, G. Palombarini, M. Carbucicchio, *J. Mater. Sci.* **39**, 933 (2004).

- [6] I. Celikyurek, B. Baksan, O. Torun, R. Gurler, *Intermetallics* **14**, 136 (2006).
- [7] M. Carbucicchio, G. Palombarini, *J. Mater. Sci. Lett.* **6**, 1147 (1987).
- [8] M. Carbucicchio, G. Palombarini, G. Sambogna, *J. Mater. Sci.* **19**, 4035 (1984).
- [9] Y. Gencer, M. Tarakci, A. Calik, *Surf. Coat. Technol.* **203**, 9 (2008).
- [10] M. Carbucicchio, G. Palombarini, G. Sambogna, *Hyperfine Interact.* **92**, 993 (1994).
- [11] G. Principi, A. Gupta, C. Badini, *Hyperfine Interact.* **69**, 479 (1991).
- [12] C.M. Brakman, A.W.J. Gommers, E.J. Mittemeijer, *J. Mater. Res.* **4**, 1354 (1989).
- [13] C. Badini, C. Gianoglio, G. Pradelli, *J. Mater. Sci.* **21**, 1721 (1986).
- [14] G. Palombarini, M. Carbucicchio, L. Cento, *J. Mater. Sci.* **19**, 3732 (1984).
- [15] M. Carbucicchio, G. Meazza, G. Palombarini, *J. Mater. Sci.* **17**, 3123 (1982).
- [16] D.K. Subramanyam, in: *ASM International Handbook*, Vol. 1, *Properties and Selection: Irons Steels and High Performance Alloys*, Materials Park (Oh) 1991 p. 1951.
- [17] M. Bektes, A. Calik, N. Ucar, M. Keddani, *Mater. Character.* **61**, 233 (2010).
- [18] H. Hermawan, D. Dube, D. Mantovani, *J. Biomed. Mater. Res. Part A* **93A**, 1 (2010).
- [19] Y.K. Lee, S.H. Baik, J.C. Kim, C.S. Choi, *J. Alloys Comp.* **355**, 10 (2003).
- [20] J.H. Jun, C.S. Choi, *Scr. Mater.* **38**, 543 (1998).
- [21] R.D. Fu, Y.Z. Zheng, Y.B. Ren, *J. Mater. Eng. Perform.* **10**, 456 (2001).